

## A Theoretical Investigation of the Pyrazole Phototransposition

Robert E. Connors,\* James W. Pavlik,\* Douglas S. Burns, and Edyth M. Kurzweil

Worcester Polytechnic Institute, Worcester, Massachusetts 01609

Received April 29, 1991

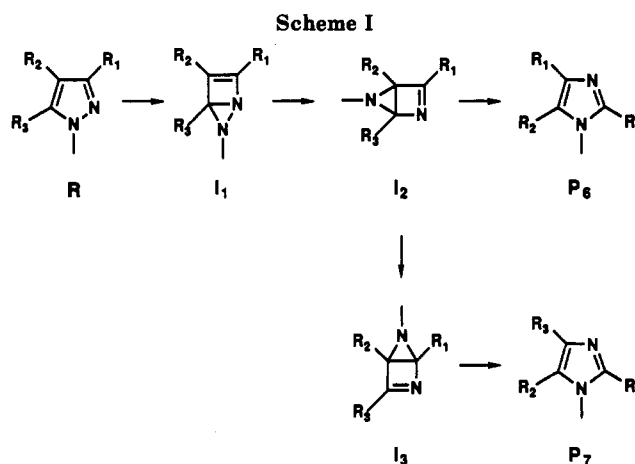
The mechanism of the phototransposition of pyrazole to imidazole was investigated using the semiempirical MO method MNDO. Potential energy surfaces were calculated for  $S_0$ ,  $S_1$ , and  $T_1$ . The heights of calculated energy barriers and the experimentally observed photoproducts suggest that the disrotatory electrocyclic ring closure forming a 1,5-diazabicyclo[2.1.0]pentene intermediate and the first [1,3]-sigmatropic shift of nitrogen occur while on an excited state surface. This is followed by internal conversion to the ground state forming a 2,5-diazabicyclo[2.1.0]pentene intermediate. At this point, the intermediate either rearomatizes to an imidazole product or undergoes a second [1,3]-shift forming another 2,5-diazabicyclo[2.1.0]pentene intermediate, which rearomatizes to a different imidazole product. MNDO calculations qualitatively support the experimentally observed product ratios of the two imidazoles that are formed for variously substituted pyrazoles.

## Introduction

The phototransposition chemistry of five-membered heterocycles has been the subject of extensive experimental<sup>1-6</sup> and theoretical studies.<sup>7-12</sup>

Work in this laboratory, for example, has shown that *N*-methylpyrazole undergoes phototransposition by three distinct permutation patterns and, accordingly, by three distinct transposition mechanisms.<sup>13</sup> These permutations can be rationalized by mechanistic pathways initiated by photolytic cleavage of the N-N bond<sup>14</sup> or by initial electrocyclic ring closure followed by one or two [1,3]-sigmatropic shifts of nitrogen. These pathways result in *N*-methylpyrazole → *N*-methylimidazole transpositions with scrambling patterns consistent with the  $P_4$ ,  $P_6$ , and  $P_7$  permutation patterns. Whereas these studies have established the gross structural changes associated with each transposition pathway, we now direct our attention to a detailed electronic description of the structural changes occurring on the ground- and excited-state transposition reaction coordinates.

The phototransposition chemistry of a variety of five-membered heterocycles has been partially or wholly rationalized by the electrocyclic ring closure-[1,3]-heteroatom shift mechanism. In the cases of thiophene<sup>10</sup> and oxazole,<sup>7</sup> ab initio calculations led to the conclusion that the [1,3]-shifts of sulfur and oxygen, respectively, occur while the molecule is on an excited energy surface. Conversely, Jug's theoretical investigations of cyanopyrrole<sup>9</sup> and thiophene<sup>12</sup> suggest that the photochemical electrocyclic ring closure is followed by a ground-state [1,3]-sigmatropic shift of nitrogen and sulfur, respectively.



In this study, the phototransposition of *N*-methylpyrazoles via the electrocyclic ring closure-nitrogen walk pathways has been investigated using computational techniques. The results obtained have been compared to the results of our experimental studies in order to better understand how *N*-methylpyrazoles transpose to *N*-methylimidazoles via this mechanistic pathway.

## Method of Calculation

All calculations were carried out using the MOPAC<sup>15</sup> program and the MNDO Hamiltonian<sup>16</sup> with standard parameters. The reliability of the MNDO method for geometries and energies of ground-state nitrogen containing compounds has been documented.<sup>17,18</sup> Recent studies have demonstrated that MNDO and MOPAC can produce meaningful information about excited-state potential energy surfaces.<sup>19-21</sup> Geometries for reactants, products, and intermediates were fully optimized using the Davidson-Fletcher-Powell minimization technique and internal coordinates. Transition structures, located with SADDLE calculations,<sup>22</sup> were refined by minimizing the scalar gradient of energy with respect to the geometry and characterized as saddle points by diagonalizing the Hessian (force constant) matrix<sup>23</sup> and establishing

(1) Barltrop, J. A.; Day, A. C.; Mack, A. G.; Shahrisa, A.; Wakamatsu, S. *J. Chem. Soc. Chem. Commun.* 1981, 604.

(2) Saito, I.; Murii, T.; Okumura, Y.; Mori, S.; Yamaguchi, K.; Matsuura, T. *Tetrahedron Lett.* 1986, 27, 6385.

(3) Barltrop, J. A.; Day, A. C.; Ward, R. W. *J. Chem. Soc., Chem. Commun.* 1978, 131.

(4) Barltrop, J. A.; Day, A. C.; Moxon, P. D.; Ward, R. W. *J. Chem. Soc., Chem. Commun.* 1975, 786.

(5) Hiraoka, J.; Srinivagan, R. *J. Am. Chem. Soc.* 1968, 90, 2720.

(6) Rendall, W. A.; Clement, A.; Torres, M.; Strausz, O. P. *J. Am. Chem. Soc.* 1986, 108, 1691.

(7) Tanaka, H.; Matsushita, T.; Nishimoto, K. *J. Am. Chem. Soc.* 1983, 105, 1753.

(8) Tanaka, H.; Osamura, Y.; Matsushita, T.; Nishimoto, K. *Bull. Chem. Soc. Jpn.* 1981, 54, 1293.

(9) Behrens, S.; Jug, K. *J. Org. Chem.* 1990, 55, 2288.

(10) Matsushita, T.; Tanaka, H.; Nishimoto, K.; Osamura, Y. *Theor. Chim. Acta* 1983, 63, 55.

(11) Buss, S.; Jug, K. *J. Am. Chem. Soc.* 1987, 109, 1044.

(12) Jug, K.; Schluff, H. *J. Org. Chem.* 1991, 56, 129.

(13) Pavlik, J. W.; Kurzweil, E. M. *J. Org. Chem.*, previous paper in this issue.

(14) Padwa, A. *Rearrangements in Ground and Excited States*; de Mayo, P., Ed.; Academic Press: New York, 1980; Vol. 3; p 501.

(15) Available from the Quantum Chemistry Program Exchange: Stewart, J. J. P. QCPE 455, v. 5.

(16) Dewar, M. J. S.; Thiel, W. *J. Am. Chem. Soc.* 1977, 99, 4899.

(17) Dewar, M. J. S.; Thiel, W. *J. Am. Chem. Soc.* 1977, 99, 4907.

(18) Olivella, S.; Vilarrasa, J. *J. Heterocycl. Chem.* 1981, 18, 1189.

(19) Troe, J.; Weitzel, K.-M. *J. Chem. Phys.* 1988, 88, 7030.

(20) Halpern, A. M.; Ruggles, C. J.; Ames, A. *J. Phys. Chem.* 1989, 93, 3448.

(21) Ames, A. E.; Halpern, A. M.; Ruggles, C. J. *J. Phys. Chem.* 1990, 94, 4464.

(22) Dewar, M. J. S.; Healy, E. F.; Stewart, J. J. P. *J. Chem. Soc., Faraday Trans. 2* 1984, 80, 227.

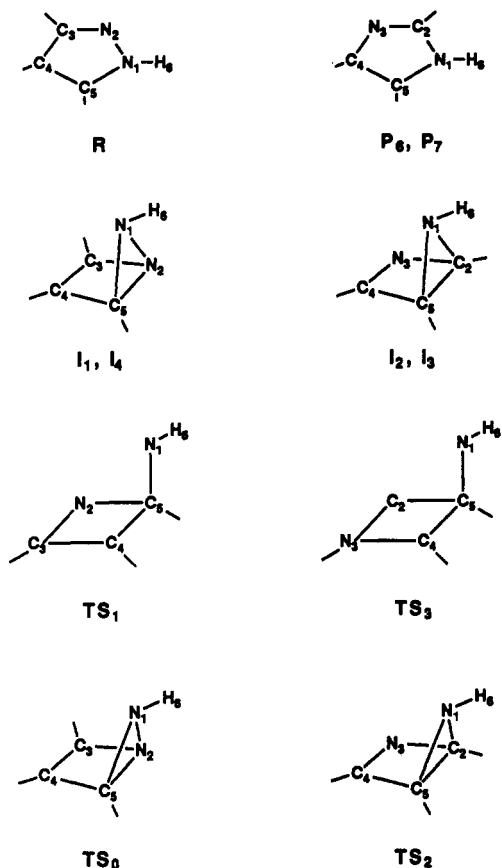


**Figure 1.** Geometry and numbering scheme of pyrazole, imidazole, intermediates, and transition structures.

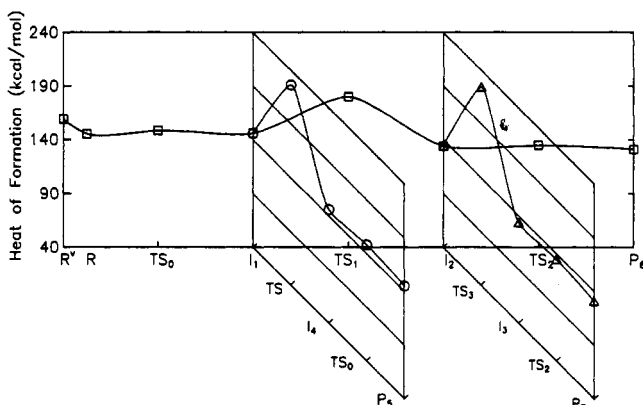


**Figure 2.**  $S_1$  potential energy surface for the phototransposition of pyrazole to  $P_5$  pyrazole,  $P_6$  imidazole, and  $P_7$  imidazole.

the presence of one and only one negative force constant.

It was not possible to minimize gradients of the transition structures for any of the species studied on the  $S_1$  potential energy surface. As a result,  $S_1$  transition structures were obtained from SADDLE calculations, which provide an approximate transition structure between two intermediates.  $S_0$  and  $T_1$  transition structures were successfully refined with gradient-minimization techniques and were characterized as transition structures with force constant calculations.

In order to simplify the calculations presented here, the unsubstituted pyrazole was used for computing the potential energy surfaces in Figures 2–4, whereas the experimental data are for *N*-methyl-substituted compounds. We have calculated major portions of these potential energy surfaces for *N*-methylpyrazole and find that they differ from the pyrazole results by a nearly constant amount of energy; therefore, conclusions derived from the unsubstituted case should be applicable to the experimental

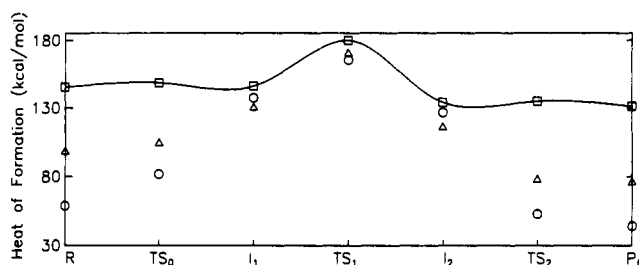


**Figure 3.** Energies of  $S_1$  optimized geometries indicated with squares. Energies calculated for  $T_1$  and  $S_0$  states using  $S_1$  optimized geometries indicated with triangles and circles, respectively.

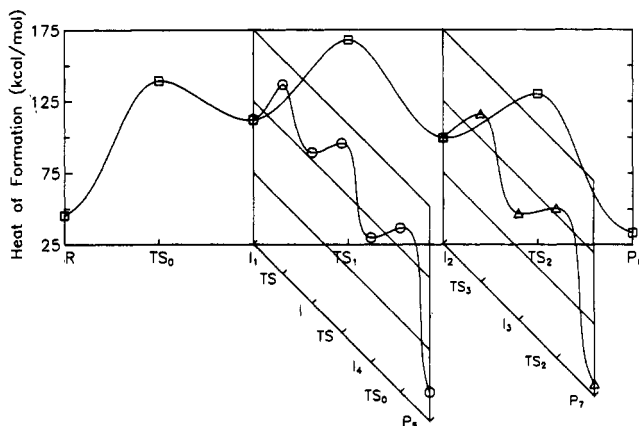


**Figure 4.**  $S_0$  potential energy surface for the phototransposition of pyrazole to  $P_5$  pyrazole,  $P_6$  imidazole, and  $P_7$  imidazole.

work. Theoretical results that are reported in Table III have been calculated for the complete molecular structure listed.

Calculations of excitation energies and oscillator strengths were also carried out using the HAM/3<sup>24</sup> semiempirical MO method with configuration interaction. The following notations are used. Pyrazole in the ground state is denoted by  $R(S_0)$ . Vertical excitations of pyrazole are denoted by  $R^v(S_1)$ ,  $R^v(S_2)$ , etc. Relaxed bicyclic intermediates are denoted as  $I_1(x)$ ,  $I_2(x)$ ,  $I_3(x)$ , and  $I_4(x)$ , where  $x$  represents the state of the molecule,  $S_0$ ,  $S_1$ , or  $T_1$ . Consistent with the permutation pathway by which they are formed, the three possible products investigated in this work are denoted as  $P_5$  (pyrazole),  $P_6$  (imidazole), and  $P_7$  (imidazole).<sup>13</sup> Transition structures are defined by  $TS_1(x)$ ,  $TS_2(x)$ , etc.

## Results and Discussion

**1. Optimized Geometries.** Pyrazole ( $R$ ), 1,5-diazabicyclo[2.1.0]pentene ( $I_1$  and  $I_4$ ), 2,5-diazabicyclo[2.1.0]pentene ( $I_2$  and  $I_3$ ), and imidazole ( $P_6$  and  $P_7$ ) were fully optimized on ground- and excited-state potential energy surfaces. Figure 1 illustrates the geometry and the numbering scheme for the intermediates and transition structures.<sup>25</sup> Pyrazole and imidazole are planar with  $C_s$  symmetry in the ground state, however the  $S_1$  and  $T_1$  symmetry geometries are nonplanar. Endo and exo conformers of each bicyclic intermediate exist, and these calculations reveal that the exo form is thermodynamically more stable for  $I_1(S_0, S_1, \text{ and } T_1)$  by 3 kcal/mol, whereas the endo form is thermodynamically slightly more stable for  $I_2(S_0, S_1)$ .

**2. Vertical Excitation of Pyrazole.** In the following sections it will be shown that it is not necessary to involve excited states higher than  $S_1$  and  $T_1$  to explain the photochemistry that is observed. The results of HAM/3-CI

(24) Åsbrink, L.; Fridh, C.; Lindholm, E. *Chem. Phys. Lett.* 1977, 52, 63–68, 69–71.

(25) A table showing computed geometric parameters for all structures is available from the authors.

(23) McIver, J. W.; Komornicki, A. *J. Am. Chem. Soc.* 1972, 94, 2625.

Table I. Vertical Excitation Wavelengths (nm) of Pyrazole

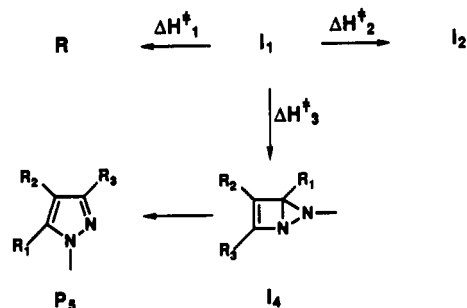
state	excitation	wavelength (nm)	oscillator strength
R <sup>v</sup> (S <sub>1</sub> )	π-π*	204	0.12
R <sup>v</sup> (S <sub>2</sub> )	n-π*	192	0.016
R <sup>v</sup> (S <sub>3</sub> )	π-π*	187	0.25
R <sup>v</sup> (S <sub>4</sub> )	π-π*	158	0.78

calculations presented in Table I show that pyrazole can reach S<sub>1</sub> by direct irradiation due to the reasonably large oscillator strength of the S<sub>1</sub> ← S<sub>0</sub> transition.<sup>26</sup> These results differ from those obtained for cyanopyrrole, whose excitation was predicted to be to S<sub>4</sub>.<sup>9</sup> The excitation of pyrazole is π-π\* type with a calculated oscillator strength of 0.12, which is in good agreement with values we calculate from published solution-phase spectra.<sup>27</sup>

The calculated excitation wavelengths are also in good agreement with experiment. S<sub>1</sub> ← S<sub>0</sub> is predicted to occur at λ = 204 nm with HAM/3 and at 251 nm with MNDO. Swaminathan measured the absorption of pyrazole in various solvents and obtained values for λ<sub>max</sub> between 206 and 210 nm depending on the solvent. The absorption red shifts with increasing solvent polarity, which is consistent with the π-π\* nature of the transition. Experimentally, the n-π\* state has not been observed; however, this is not unreasonable since the weak n-π\* absorption may be buried beneath the nearby π-π\* transition.<sup>28</sup>

**3. S<sub>1</sub> Potential Energy Surfaces.** The reactants, products, and intermediates were initially optimized on the S<sub>1</sub> potential energy surface. SADDLE calculations were carried out between each set of intermediates along the reaction coordinate in order to determine the height of the energy barriers. Since there are two conformations of the bicyclic intermediates, SADDLE calculations were performed between all combinations of the conformers of I<sub>1</sub> and I<sub>2</sub>. In all cases, the transition structures are within a few kcal/mol of each other.

The S<sub>1</sub> potential energy surface for the phototransposition of pyrazole to imidazole via the P<sub>6</sub> and P<sub>7</sub> pathways and for the P<sub>5</sub> pyrazole to pyrazole transposition following the proposed walk mechanism is illustrated in Figure 2. Pyrazole, R(S<sub>0</sub>), absorbs a photon and is excited to its S<sub>1</sub> energy state, R<sup>v</sup>(S<sub>1</sub>). The N<sub>1</sub>-N<sub>2</sub> bond length increases from 1.33 to 1.42 Å upon relaxation to R(S<sub>1</sub>). This indicates a weakening of the N-N bond in pyrazole. In forming the relaxed excited-state pyrazole, planarity is lost and N<sub>1</sub> moves out of plane by 13°. These calculations thus reveal that the geometry of the S<sub>1</sub> relaxed pyrazole, from which it undergoes disrotatory electrocyclic ring closure, is approaching the geometry of the exo form of the 1,5-diazabicyclo[2.1.0]pentene intermediate I<sub>1</sub>(S<sub>1</sub>). In the case of I<sub>1</sub>(S<sub>1</sub>), the nitrogen is approximately 55° above the plane of the molecule. Furthermore, the calculated changes in internuclear distances are consistent with N<sub>2</sub>-C<sub>5</sub> bond formation as a result of electrocyclic ring closure. Thus, this distance decreases continuously from 2.28 Å in R(S<sub>1</sub>) to 2.10 and 1.88 Å in TS<sub>0</sub>(S<sub>1</sub>) and I<sub>1</sub>(S<sub>1</sub>), respectively. While on the S<sub>1</sub> surface, a [1,3]-sigmatropic shift of nitrogen takes place in which the aziridine nitrogen atom walks away from the nitrogen of the four-membered ring. During this nitrogen shift, the N<sub>2</sub>-C<sub>5</sub> bond of I<sub>1</sub>(S<sub>1</sub>) strengthens as the bond distance decreases from 1.88 to 1.51 to 1.43 Å in transforming from I<sub>1</sub>(S<sub>1</sub>) to TS<sub>1</sub>(S<sub>1</sub>) to

Figure 5. Possible pathways for reaction from I<sub>1</sub>.

I<sub>2</sub>(S<sub>1</sub>). This is reasonable since the N<sub>2</sub>-C<sub>5</sub> bond of I<sub>1</sub> is no longer part of the highly strained three-membered ring in I<sub>2</sub>. Furthermore, during the [1,3]-shift, the N<sub>2</sub>-C<sub>3</sub> single bond of I<sub>1</sub> is transformed into a double bond in I<sub>2</sub>. This is consistent with the decrease in bond length from 1.41 to 1.32 Å on S<sub>1</sub>. Upon formation of the 2,5-diazabicyclo[2.1.0]pentene intermediate I<sub>2</sub>, the molecule could, if it were to remain on S<sub>1</sub>, rearomatize forming an imidazole which is consistent with the P<sub>6</sub> permutation pattern, or it could undergo a second [1,3]-shift before rearomatization to an imidazole consistent with the P<sub>7</sub> permutation pattern. Rearomatization of I<sub>2</sub> and I<sub>3</sub> to the P<sub>6</sub> and P<sub>7</sub> imidazoles, respectively, is accompanied by an increase in the C<sub>2</sub>-C<sub>5</sub> bond distance from 1.86 to 2.22 Å on S<sub>1</sub>. In addition, N<sub>1</sub> returns to the plane of the molecule after being 54° above the plane in I<sub>2</sub> and I<sub>3</sub>. It is also conceivable that at I<sub>1</sub>, the nitrogen could walk in the opposite direction forming a second 1,5-diazabicyclo[2.1.0]pentene intermediate I<sub>4</sub>, which would rearomatize to a pyrazole consistent with the P<sub>5</sub> permutation pattern.

In order to locate likely cross-over pathways from S<sub>1</sub> to lower energy state surfaces, T<sub>1</sub> and S<sub>0</sub> energies were calculated using the S<sub>1</sub> optimized geometries and are shown in Figure 3. These data show that the potential energy surfaces come very close together at the bicyclic intermediates. The return to the ground state via radiationless transition may occur at I<sub>1</sub>(S<sub>1</sub>), prior to the [1,3]-shift of nitrogen, or at I<sub>2</sub>(S<sub>1</sub>), after the walk has occurred. The equilibrium geometries of the bicyclic intermediates on S<sub>1</sub> correspond very closely to the transition structures for rearomatization on S<sub>0</sub>. In comparing I<sub>1</sub>(S<sub>1</sub>) and TS<sub>0</sub>(S<sub>0</sub>), the corresponding interatomic distances are within 0.02 Å, bond angles are within 1.7°, and dihedral angles are within 1.5°. Since the relaxed potential energy surfaces are calculated to be less than 8 kcal/mol apart at these points, radiationless transfer from S<sub>1</sub> to S<sub>0</sub> is expected to be quite fast due to favorable Franck-Condon factors.

**4. Pyrazole-Imidazole (P<sub>6</sub>) Phototransposition Path.** The S<sub>1</sub> and S<sub>0</sub> potential energy surfaces are shown in Figures 2 and 4, respectively, where all points correspond to optimized geometries. Upon absorption of a photon of light, pyrazole is excited vertically to S<sub>1</sub> followed by rapid relaxation to its equilibrium geometry where it undergoes electrocyclic ring closure to form the 1,5-diazabicyclo[2.1.0]pentene intermediate I<sub>1</sub>(S<sub>1</sub>). Upon formation of I<sub>1</sub>(S<sub>1</sub>), various possibilities for reaction exist. First, since the S<sub>1</sub> and S<sub>0</sub> potential energy surfaces are very close at I<sub>1</sub>(S<sub>1</sub>) (Figure 3), this geometry should represent a likely cross-over point for an I<sub>1</sub>(S<sub>1</sub>) to I<sub>1</sub>(S<sub>0</sub>) radiationless transition to occur.

Upon formation of I<sub>1</sub>(x), where x can be S<sub>1</sub>, T<sub>1</sub>, or S<sub>0</sub>, three possibilities for reaction exist. The three pathways are illustrated in Figure 5 and are described as follows. First, I<sub>1</sub> may rearomatize and return to the reactant (R). Second, the aziridine nitrogen may walk away from nitrogen in the four-membered ring and form the I<sub>2</sub> inter-

(26) INDO/S-CI calculations also assign π-π\* absorption to S<sub>1</sub> with an oscillator strength of 0.102. However, INDO/S inverts the order of S<sub>2</sub> and S<sub>3</sub> from those reported by HAM/3-CI with S<sub>2</sub> (π,π\*) and S<sub>3</sub> (n,π\*).

(27) Swaminathan, M.; Dogra, S. K. *Ind. J. Chem.* 1983, 22A, 853-857.

(28) Mason, S. F. *Physical Methods in Heterocyclic Chemistry*; Kartzky, A. R., Ed.; Academic Press: New York, 1963; Vol. 2, p 60.

**Table II. Activation Enthalpies (kcal/mol) for Reaction from  $I_1(x)$  and  $I_2(x)$** 

reaction	$x = S_0$	$x = S_1$	$x = T_1$
$I_1(x) - R(x)$	29	3	3
$I_1(x) - I_2(x)$	56	31	17
$I_1(x) - I_4(x)$	45	81	51
$I_2(x) - I_1(x)$	69	46	
$I_2(x) - I_3(x)$	43	90	
$I_2(x) - P_6(x)$	30	1	

mediate. The third possibility is that the aziridine nitrogen may walk toward the nitrogen in the four-membered ring and form  $I_4$ . Competition among these three processes is governed by the relative heights of the energy barriers involved. Activation enthalpies for each pathway are summarized in Table II for unsubstituted pyrazole. The energy barriers for  $S_1$  and  $S_0$  are shown on the potential energy surfaces in Figures 2 and 4.

The activation enthalpies shown in Table II suggest that, of the ground-state pathways available to  $I_1(S_0)$ , conversion back to the reactant pyrazole should occur with the fastest rate. Furthermore, since the activation enthalpy  $\Delta H^*_3$  is 11 kcal/mol lower than  $\Delta H^*_2$ , on the ground state, the rate of  $P_5$  pyrazole formation should be substantially faster than the rate of imidazole formation via the  $P_6$  pathway. This conclusion is not consistent with the experimental observations, which clearly confirm the absence of pyrazole  $\rightarrow$  pyrazole transposition. Accordingly, it is reasonable to conclude that the first [1,3]-sigmatropic shift is not a ground-state process and that radiationless crossing at  $I_1(S_1)$  to  $I_1(S_0)$  would be an energy-wasting process leading only to the reactant pyrazole,  $R(S_0)$ .<sup>29</sup>

Further examination of Table II, however, reveals that on either the  $S_1$  or  $T_1$  reaction coordinate, the energy barrier for formation of  $I_2$ , which upon rearomatization forms the  $P_6$  imidazole, is calculated to be substantially lower than for formation of  $I_4$ , which upon rearomatization forms the  $P_5$  pyrazole. On the  $S_1$  surface, for example,  $\Delta H^*_2$  is predicted to be 50 kcal/mol less than  $\Delta H^*_3$ , indicating that the rate of the  $P_5$  pyrazole  $\rightarrow$  pyrazole transposition would not be competitive with the rate of the  $P_6$  pyrazole  $\rightarrow$  imidazole pathway. Since this is consistent with our experimental observation, we conclude that the first nitrogen walk is an excited-state process, occurring presumably from the  $S_1$  state,<sup>30</sup> leading to the formation of  $I_2(S_1)$ .

The  $S_1$  activation enthalpies shown in Table II indicate very high energy barriers for either the reverse  $I_2(S_1) \rightarrow I_1(S_1)$  or the forward  $I_2(S_1) \rightarrow I_3(S_1)$  sigmatropic shifts. Conversely, as expected from symmetry considerations, Table II shows that electrocyclic ring opening of  $I_2(S_1)$  to yield the excited singlet state of the  $P_6$  imidazole is a very facile process. It is of interest to note, whereas Figure 3 shows that the  $S_1$ - $S_0$  energy gap is small at  $I_2$ , thus predicting that the internal conversion from  $I_2(S_1)$  to the  $S_0$  surface is likely, the  $S_1$ - $S_0$  energy gap at the  $P_6$  imidazole is large consistent with inefficient radiationless decay of  $S_1$  imidazole to the ground-state product. It seems likely that the molecule undergoes rapid ring opening-ring closing until it undergoes radiationless transition from  $I_2(S_1)$  to  $I_2(S_0)$ .

As shown in Figure 4 and Table II,  $I_2(S_0)$  may either rearomatize to the  $P_6$  imidazole with an activation enthalpy

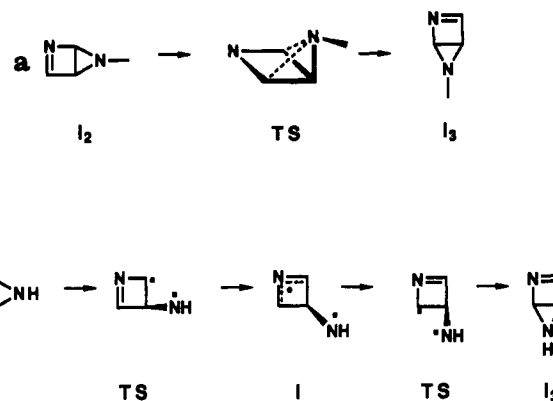


**Figure 6.** (a) Concerted scheme for nitrogen walk from  $I_2$  to  $I_3$ . (b) Biradial scheme for nitrogen walk from  $I_2$  to  $I_3$ .

of 30 kcal/mol or it may undergo a nitrogen walk and form a second 2,5-diazabicyclo[2.1.0]pentene intermediate  $I_3(S_0)$  with an activation enthalpy of 43 kcal/mol before rearomatization to the  $P_7$  imidazole. It is unlikely that  $I_1$  can be formed from  $I_2$  via [1,3]-sigmatropic shift of nitrogen while on the  $S_0$  surface, since the activation enthalpy is 26 kcal/mol larger than that for formation of  $I_3$  via walk of nitrogen on  $S_0$ . Furthermore,  $I_1(S_0)$  is thermodynamically less stable than  $I_2(S_0)$  by approximately 10 kcal/mol.

**5. Concerted vs Biradical Mechanisms.** The possibility of biradical involvement in the rearomatization of  $I_2(S_0)$  to the  $P_6$  imidazole and in the walk of  $I_2(S_0)$  to  $I_3(S_0)$  was investigated. Closed-shell potential energy surfaces, as presented in Figure 4, were calculated for both mechanisms. The potential energy surfaces for rearomatization and [1,3]-shift were then recalculated with inclusion of limited configuration interaction (CI). Upon inclusion of CI, the energies of all intermediates in the reaction mechanism changed by less than 4 kcal/mol while the geometry remained virtually the same. Therefore, these structures are nonbiradicaloid, and the energy is taken to be that calculated without CI.

The rearomatization of  $I_2(S_0)$  to the  $P_6$  imidazole proceeds via disrotatory electrocyclic ring opening<sup>31</sup> due to steric reasons and is considered to be a forbidden (in the Woodward-Hoffmann sense) concerted process. The transition structure for rearomatization to the  $P_6$  imidazole  $TS_2(S_0)$  could only be optimized as a closed-shell molecule and could not be located using CI, suggesting that a biradical structure may not exist between the two closed-shell intermediates. Biradical calculation stabilized the energy of the closed-shell geometry of transition structure  $TS_2(S_0)$  by 17.5 kcal/mol; however, geometry optimization with CI of the closed-shell transition structure caused rearrangement to the  $P_6$  imidazole product. It has been argued that biradical energies are calculated to be too low by about 15 kcal/mol because electron correlation has already been accounted for in the parameterization of MNDO and is overcompensated for when CI is included in the calculation.<sup>32</sup> Therefore, we conclude that there is not sufficient stabilization in the energies of the molecules using CI to suggest biradical involvement in the reaction mechanism.

Results of the investigation of the [1,3]-sigmatropic shift of nitrogen from  $I_2(S_0)$  to  $I_3(S_0)$  are not as conclusive as in the rearomatization case. Potential energy surfaces were

(29) Preliminary calculations suggest that substituents can alter the  $S_1$ - $S_0$  energy gap at  $I_1$  and hence the rate of radiationless crossing before the 1,3-sigmatropic shift occurs. Further studies are in progress.

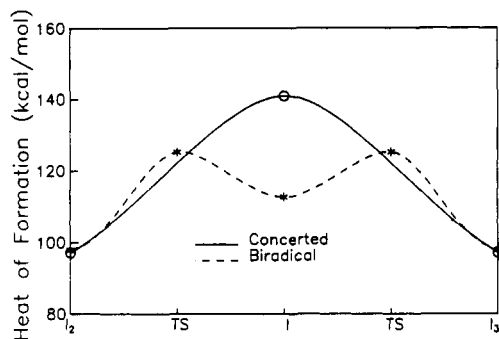
(30) Attempts to sensitize or quench the transposition with triplet sensitizers or quenchers have been unsuccessful.

(31) Woodward, R. B.; Hoffmann, R. *The Conservation of Orbital Symmetry*; Verlag Chemie: Weinheim, 1971.

(32) Dewar, M. J. S.; Fox, M. A.; Campbell, K. A.; Chen, C. C.; Friedheim, J. E.; Holloway, M. K.; Kim, S. C.; Liescheski, P. B.; Pakiari, A. M.; Tien, T. P.; Zebisch, E. G. *J. Comput. Chem.* 1984, 5, 480.

Table III. Summary of  $P_6$  vs  $P_7$  Data

reactant	$\Delta H^*_A$ (kcal/mol)	$\Delta H^*_B$ (kcal/mol)	$\Delta(\Delta H^*)$ (kcal/mol)	$\Delta H_r$ (kcal/mol)	observed ( $P_4/P_6/P_7$ )
3-cyano-1,5-dimethylpyrazole <sup>a</sup>	29.7	31.8	2.1	-1.53	4.6/1.6/1
1,5-dimethylpyrazole	29.8	36.7	6.9	-3.30	3.5/1.8/1
<i>N</i> -methylpyrazole	30.6	39.5	8.9	0	4.9/7.2/1
3-cyano-1-methylpyrazole <sup>a</sup>	31.8	35.6	3.8	1.71	2.3/1/-
1,3-dimethylpyrazole	33.2	40.0	6.8	3.30	1.6/1/-
1,4-dimethylpyrazole	29.0	39.2	10.2	0	only $P_4$
pyrazole	30.1	43.6	13.5	0	

<sup>a</sup> Reference 1.Figure 7. Concerted and biradical potential energy surfaces for the nitrogen walk from  $I_2(S_0)$  to  $I_3(S_0)$ .

calculated for closed-shell and biradical mechanisms. The two mechanisms are illustrated in Figure 6a,b, and the corresponding potential energy surfaces are compared in Figure 7. In considering all of the combinations of the two conformers of the bicyclic intermediates  $I_2$  and  $I_3$ , the lowest energy barrier for walking following a concerted process is 44 kcal/mol, whereas the barrier for a biradical mechanism is 28 kcal/mol. In the concerted pathway the transition structure  $TS_3(S_0)$  possesses a plane of symmetry perpendicular to the plane of the four-membered ring. The  $C_4-C_5$  and  $C_2-C_5$  bond lengths are equal (1.53 Å), as are the  $C_2-N_3$  and  $C_4-N_3$  bond lengths (1.38 Å). Also, the migrating nitrogen,  $N_1$ , is situated directly above  $C_5$  as shown by the  $N_3-C_2-C_5-N_1$  dihedral angle of 87°. However, in the biradical mechanism the molecule passes through a nonsymmetric transition structure before reaching a symmetric intermediate. It should be noted that the biradical potential energy surface is similar to that obtained by Jug<sup>9</sup> in the analysis of the photochemistry of pyrrole, a similar five-membered heterocycle. Since energies obtained with CI are expected to be too low by approximately 15 kcal/mol as previously discussed, these predicted barriers of biradical and concerted mechanisms may not be very different. At the MNDO level, it is difficult to distinguish between the two pathways. The mechanism may be biradical, but the true energy barrier probably lies between the values calculated for the closed-shell and biradical cases.

**6. Comparison of MNDO with Experiment.** Calculations suggest that the second [1,3]-sigmatropic shift is a ground-state process. In order to test this possibility, ground-state potential energy surfaces have been calculated for several molecules for which experimental data exists. Qualitative support for the observed  $P_6$  imidazole to  $P_7$  imidazole relative product distributions has been obtained from the calculations by a combination of thermodynamic and kinetic considerations. Table III is a summary of the experimental data and the calculated results for several molecules following the scheme shown in Figure 8.  $P_4$  corresponds to the phototransposition product that is obtained via the proposed ring contraction-ring expansion mechanism.<sup>13,33</sup>

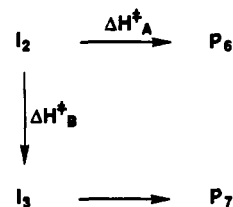


Figure 8. Scheme for analysis of Table III.

In Table III,  $\Delta H^*_A$  is the activation enthalpy for rearomatization of  $I_2(S_0)$  to  $P_6(S_0)$  and  $\Delta H^*_B$  is the activation enthalpy for undergoing the [1,3]-sigmatropic shift to form  $I_3(S_0)$  from  $I_2(S_0)$ .  $\Delta(\Delta H^*)$  is the difference between these two values and  $\Delta H_r$  is the reaction enthalpy for  $I_2(S_0) \rightarrow I_3(S_0)$ . A dash indicates that no observable product was obtained.

Qualitatively, as the difference between  $\Delta H^*_A$  and  $\Delta H^*_B$  increases, the  $P_6/P_7$  product ratio increases. This can be seen for the first three molecules in Table III where  $\Delta(\Delta H^*)$  increases from 2.1 to 8.9 kcal/mol and the observed product ratio increases from 1.6/1 to 7.2/1. In addition, as  $\Delta H_r$  changes from exothermic to zero to endothermic, the  $P_6$  to  $P_7$  ratio increases. The first five molecules in Table III illustrate this trend with the amount of  $P_6$  to  $P_7$  products increasing to the point where no  $P_7$  imidazole is observed. A point worth noting from these data is that in cases where it seems reasonable kinetically to form the  $P_7$  imidazole, but unreasonable by thermodynamic considerations (3-cyano-1-methylpyrazole and 1,3-dimethylpyrazole), the  $P_7$  product has not been observed. In the case of 1,4-dimethylpyrazole, only the  $P_4$  imidazole product has been obtained experimentally. However, irradiation of 1,5-dimethylimidazole, the  $P_6$  product of 1,4-dimethylpyrazole, with appropriate deuterium labeling, results in an equilibrium amount of  $P_6$  and  $P_7$  imidazoles. Although the  $P_6$  to  $P_7$  product ratio is not known, the observance of both products is consistent with the kinetic and thermodynamic data of 1,4-dimethylpyrazole in Table III.

Since the [1,3]-shift of nitrogen from  $I_2$  to  $I_3$  and the rearomatization of  $I_2$  to  $P_6$  are predicted to be ground-state thermal processes and the calculated barrier for rearomatization is smaller than the barrier for the [1,3]-shift, the  $P_6$  to  $P_7$  product ratio should be sensitive to temp. changes. Consistent with this theoretical prediction, we have obsd. that photoreaction of 1,5-dimethylpyrazole at 30, 10, 0, -10, and -30 °C results in an increasing  $P_6$  to  $P_7$  product ratio but that the total amount of  $P_6$  and  $P_7$  products formed over this temperature range remains essentially constant.<sup>34</sup>

Our finding that the barrier for rearomatization is smaller than the barrier for walking in the ground state

(33) Tiefenthaler, H.; Dörschlen, W.; Goth, H.; Schmid, H. *Helv. Chim. Acta* 1967, 50, 2244.

(34) Connors, R. E.; Pavlik, J. W.; Burns, D. S.; Kurzwil, E. M. Manuscript in preparation.

is in accord with Barltrop's experimental and Jug's SINDO1 conclusions concerning cyanopyrrole. Photolysis of 1,5-dimethylpyrazole was also carried out at 77 K in frozen acetonitrile resulting in the formation of imidazoles that are consistent with only the  $P_4$  and  $P_6$  permutation patterns. No  $P_7$  imidazole was detected even after 33% of the reactant had disappeared. These observations are consistent with our calculated results, which suggest that  $I_2$  forms on a relatively flat potential energy surface, such as  $S_1$ , and that subsequent reactions occur on the ground-state surface.

### Conclusion

MNDO calculations and experimental product distributions are used to provide a qualitative explanation of the phototransposition of pyrazole to imidazole via [1,3]-sigmatropic shift of nitrogen. Initial electrocyclic ring closure of pyrazole and walk of nitrogen occur on the  $S_1$  potential energy surface. The return to the ground state is via a radiationless transition from  $I_2(S_1)$  to  $TS_2(S_0)$ . The second [1,3]-shift of nitrogen may be a biradical process;

however, it is difficult to clearly distinguish between concerted and biradical mechanisms at the MNDO level. Kinetic and thermodynamic arguments are in qualitative agreement with the experimentally observed relative product distributions of the  $P_6$  and  $P_7$  imidazoles and support the assignment of the second walk to a ground-state process. Photolysis at decreasing temperature results in increasing  $P_6$  to  $P_7$  product ratios. This is consistent with a ground-state thermal reaction and a smaller barrier for rearomatization than walking as suggested by the theoretical calculations.

**Acknowledgment.** The authors thank A. E. Johansen and the staff of the College Computing Center for their assistance during the early stages of this project. We are grateful to Professor M. C. Zerner of the University of Florida for providing a copy of his INDO program. DECstation 3100 and Encore Multimax 520 computers at Worcester Polytechnic Institute were used for the computations.

**Registry No.** R, 288-13-1;  $P_6, P_7$ , 288-32-4;  $I_1, I_4$ , 74613-28-8;  $I_2, I_3$ , 74613-34-6.

## Structures and Lifetimes of 1,4-Biradical Intermediates in the Photochemical Cycloaddition Reactions of *N*-Benzoylindole with Alkenes<sup>1</sup>

David J. Hastings and Alan C. Weedon\*

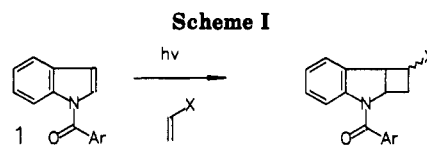
Photochemistry Unit, Department of Chemistry, The University of Western Ontario, London, Ontario, N6A 5B7, Canada

Received April 29, 1991

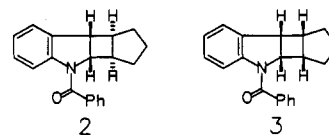
The photochemical cycloaddition reaction of *N*-benzoylindole with 1,6-heptadiene, tetramethylethylene, and vinylcyclopropane has been examined. The structures of the products suggest that the reaction proceeds via a 1,4-biradical intermediate that is formed by bonding between one terminus of the alkene and the 2-position of the indole derivative. This result is used to explain the origin of the previously observed regioselectivity of the photochemical cycloaddition reaction. The biradical intermediates obtained in the photochemical cycloaddition reaction of *N*-benzoylindole with vinylcyclopropane and 1,6-heptadiene can undergo rearrangement reactions whose rate constants can be estimated. Using these rates as clocks, the lifetimes of the intermediate biradicals in the photochemical cycloaddition reaction of *N*-benzoylindole with alkenes are estimated to be of the order of 100 ns. The consequences of this for the potential success of synthetically useful trapping of the intermediate biradicals is discussed.

### Introduction

It has been reported<sup>2,3</sup> that indoles possessing a benzoyl substituent on the nitrogen atom form cyclobutane products when irradiated with ultraviolet light in the presence of alkenes. With monosubstituted alkenes the reaction is found<sup>3</sup> to be regioselective, but not normally stereoselective, as indicated in Scheme I. This reaction offers a potential route for the synthesis of substituted indoles if methods for elaboration of the cyclobutane ring can be developed. With this as our motivation, we have been examining the mechanism of this photochemical cycloaddition reaction in order that the factors governing the reaction regiochemistry and stereochemistry can be understood. We have previously obtained<sup>4</sup> steady-state kinetic results that suggest that the reaction proceeds as shown in Scheme II. In this scheme, intersystem crossing



of the singlet excited state of *N*-benzoylindole (1) occurs efficiently<sup>5</sup> to yield the triplet excited state, which is intercepted by an alkene such as cyclopentene to give one or more isomeric 1,4-biradical intermediates. The major fates of the biradicals are reversion to the ground-state indole derivative and alkene or closure to the cyclobutane products 2 and 3. The intermediacy of biradicals that



partition between product and starting material is sup-

(1) Contribution no. 440 from the Photochemistry Unit, University of Western Ontario.

(2) Julian, D. R.; Foster, R. J. *Chem. Soc., Chem. Commun.* 1973, 311.

(3) Ikeda, M.; Ohno, K.; Mohri, S.; Takahashi, M.; Tamura, Y. *J. Chem. Soc., Perkin Trans. 1* 1984, 405.

(4) Disanayaka, B. W.; Weedon, A. C. *Can. J. Chem.* 1990, 68, 1685.

(5) Disanayaka, B. W.; Weedon, A. C. *Can. J. Chem.* 1987, 65, 245.